

## FINITE ELEMENT METHODS FOR EVALUATING OPTICAL SYSTEM PERFORMANCE

Alson E. Hatheway

Consultant, Alson E. Hatheway Inc., Consulting Engineers  
1041 East Green Street, Pasadena, California 91106

### Abstract

Many aspects of geometric optics and wave optics are compatible with the finite element method of analysis. This fact provides a new and powerful tool in the fields of optomechanical design and optical systems engineering. Using special features available in some commercially available finite element codes, it is possible to include optical system parameters as a portion of the finite element model. The simultaneous solution of the optical and mechanical problems provides higher accuracy and consistency of the results, efficient calculation of many different load cases, and solutions to optics design problems which are difficult or impossible to handle in traditional lense design codes. This paper shows results possible in commercially available finite elements codes used to calculate optical system parameters, including surface figure changes, generalized optical ray tracing and wavefront error computation. The paper is illustrated with examples drawn from recent practice.

### Introduction

The finite element method has been developed over the last fifty years as a tool to aid civil engineers and mechanical engineers in the analysis of strength and rigidity of structures. It found immediate applications in the evaluation of designs for bridges, transmission towers, tall buildings and airframes. The development of high speed digital computers has made the analysis of large structural problems a routine and economical activity. Many people view the finite element method as being uniquely linked to digital computers and stress analysis of structures. Both impressions are false.

The development of the finite element method predates the digital computer by many years. In the early days the finite element problems were solved on analog computers which assembled resistors, capacitors, inductors, and other components, into a network which simulated the structure according to a set of laws called "The Electrical-Mechanical Analogy." It is only comparatively recently that large scale problems have become economical on digital computers. This economic shift to digital solution has been brought about by the dramatic reduction in the cost of computer time as well as the development of fast and accurate matrix solution methods. None the less, today's finite element methods owe an enormous debt to the developers and operators of the early analog methods.

Early finite element work was energized by the structural analysis arts. The prospect of being able to solve large complex structures which could be rigorously described as an assemblage of much smaller known solutions to yield a reliable and provably accurate solution opened the door for projects and products which had only been dreams for want of economical computational procedures. But, if in acknowledging the development of structural analysis methods, we are satisfied, we will over look an enormous legacy that the finite element pioneers have left for us.

This legacy consists of the methods for economically solving large numbers of simultaneous algebraic and differential equations. It is true that most of the effort has gone into solving structural equations of one form or another. But in recent years, heat transfer and fluid mechanics have been added to the repertoire of most finite element codes. In reality the method doesn't care what kind of problem it is solving, as long as the form of the equations is familiar. Although it is possible to organize problems of many kinds (electrical and magnetic fields, orbital mechanics, hydraulics, etc.) we will limit our discussion here to optical and optomechanical problems.

### Organizing the optical laws

The laws of reflection and refraction (Snell's Law) are readily organized into finite element codes. Since the writer works predominantly with the MSC/NASTRAN code the following remarks are couched in the jargon of MSC/NASTRAN and users of other codes may need to make the appropriate translations before applying these remarks to their problems.

The laws of reflection (Figure 1) and refraction (Figure 2) relate the angle of depart-

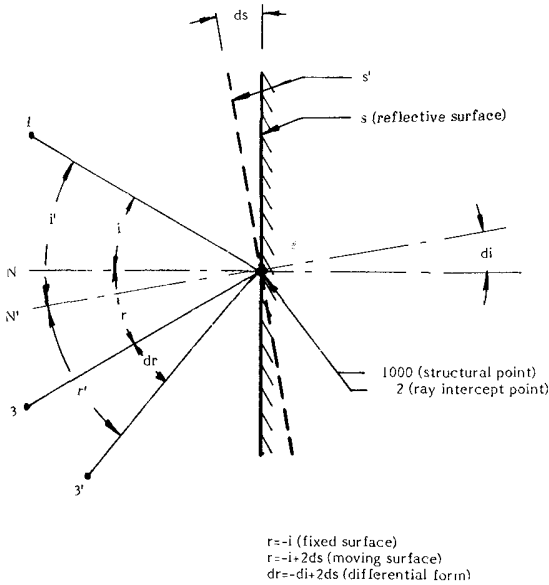


Figure 1. The law of reflection.

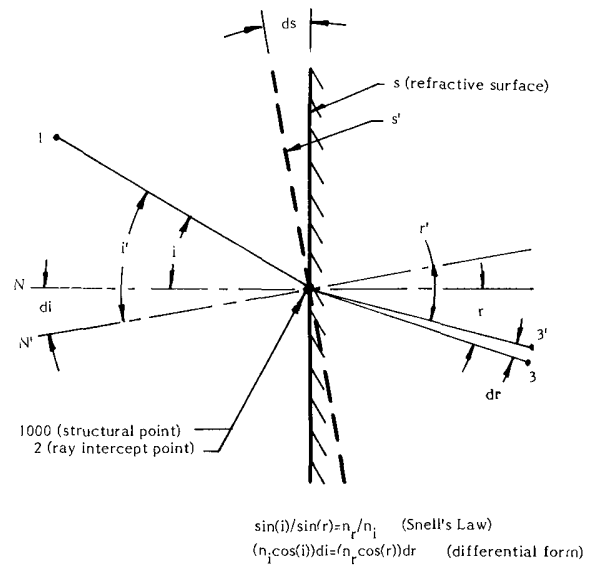


Figure 2. The law of refraction (Snell's Law).

ure (reflection or refraction) to the angle of the incidence and the geometric and material properties at the intercept point. Since the code allows us to manipulate degrees of freedom only in the "displacement vector" it is the first derivative of the optical laws that we will apply. In taking the derivatives and re-arranging these laws we will see that constant co-efficients are definable which can be used to define the motion of the departing ray based upon the incident ray's motions and motions of the surface at the point of intercept. These equations can be re-arranged for coding onto MPC (Multipoint Constraint) cards in the MSC/NASTRAN code (See Figures 3 and 4). By coding all six degrees of freedom of

$dr = -di + 2ds$   
 Or, if the ray from GRID 1 is fixed in space,  
 $dr = 2ds$   
 Reformatted for an MPC card and using the notation of Figure 1,  
 $d(2) - 2d(1000) = 0,$   
 and,

MPC	SID	2	6	1 0	1000	6	-2 0		
-----	-----	---	---	-----	------	---	------	--	--

Figure 3. MSC/NASTRAN Data Card for the law of reflection.

$(n_i \cos(i))ds = (n_r \cos(r))dr,$   
 or,  
 $dr = (n_i/n_r) \cos(i)/\cos(r) ds.$   
 Reformatted for an MPC card and using the notation of Figure 2,  
 $d(2) - (n_i/n_r) \cos(i)/\cos(r) d(1000) = 0,$   
 and,

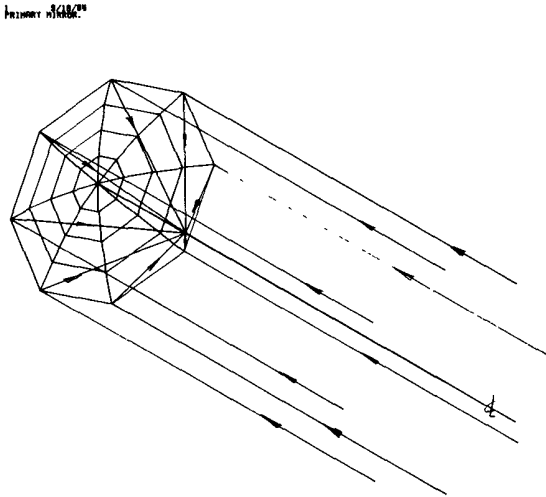
MPC	SID	2	6	1 0	1000	6	$(n_i/n_r) \cos(i)/\cos(r)$		
-----	-----	---	---	-----	------	---	-----------------------------	--	--

Figure 4. MSC/NASTRAN Data Card for the law of refraction (Snell's Law).

each ray intercept point, we can control the position and orientation of each ray intercept point in accordance with the first derivative of the laws of geometric optics. We can thereby trace a ray through a system from object to image. If the analysts job is well done, the resulting ray trace will respond accurately to all disturbances of the structure,

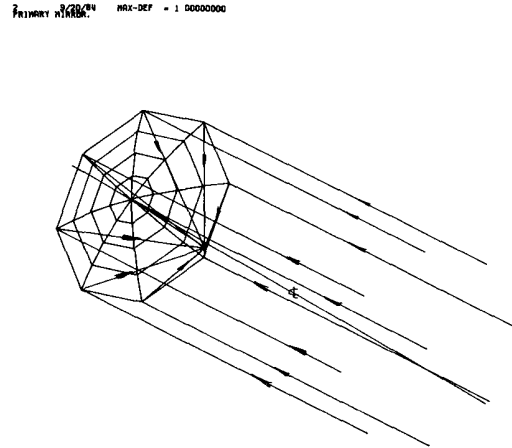
as well as motion of the object when the structure is undisturbed.

A simple example of ray tracing is shown in Figure 5. A parabolic mirror (f/1.6) is illuminated with axial collimated light. The light comes to a focus as expected. If the axial illumination is shifted off axis as in Figure 6, the focal point shifts off axis by



OPTICAL DESIGN  
UNDEFORMED SHAPE

Figure 5. MSC/NASTRAN Model of f/1.6 parabolic mirror with axial illumination.



OPTICAL DESIGN  
STATIC DEFOR SUBCASE 1 LOAD 1

Figure 6. Parabolic mirror with off-axis illumination.

the appropriate amount. Furthermore, if one examines the off axis image of the point source, one sees a familiar aberration, coma (Figure 7). At this point the analyst needs

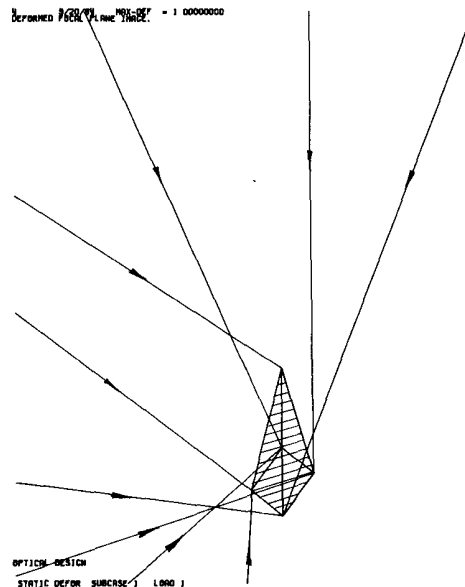


Figure 7. MSC/NASTRAN forms a comatic image with off-axis illumination.

to check the numerical output data. Not only should the focus be offset by the proper amount but the proportions of the comatic image should be appropriate for the optical system. There have been no simplifying assumptions or approximations put into the model.

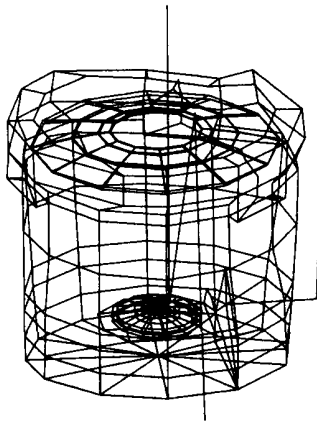
Wave front errors are evaluated by computing the change in propagation lengths for a number of rays which pass through the system. The methods for calculating the path length changes are similar to the general ray tracing methods described above. Interferograms

and test plate patterns may be used to assess surface figure changes caused by any combination of loads on the optical system. These techniques use rigid elements to form a test plate which moves with the optical surface and removes the bulk motion of the surface itself. The resulting airgap between the rigid elements and the deformed optical surface is then contour plotted. By selecting the appropriate half-wavelengths as the interval for the contours, the plots will be accurate representations of test plate patterns or interferograms observed under illumination of the selected wavelength. A more detailed discussion of the coding procedures for all of these techniques is presented elsewhere.<sup>1</sup>

### Cassegrainian afocal telescope

Our first example of the use of these techniques is a Cassegrainian afocal telescope attachment. It was required that the optical performance not be impaired by mounting it to a dirty or damaged surface. The mounting flange deformation is obvious in Figure 8. Chief ray calculation and a surface figure plot of the primary mirror (Figure 9) indicate that

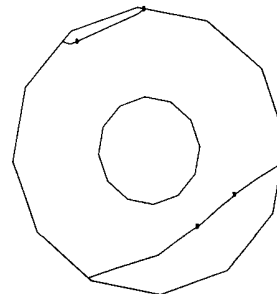
7/23/65 HRL-207 - 0.0000000



100% HE NE LASER ILLUMINATION  
STATIC DEFOR. SURFACE 1 LAMB 300

Figure 8. Deformed flange on a Cassegrainian afocal telescope attachment.

15 7/23/65 HRL-207 - 0.0000000



SYMBOL	VALUE (INCHES)	SYMBOL	VALUE (INCHES)
1	5.00E-05	15	-1.25E-04
2	3.75E-05	16	1.38E-04
3	2.50E-05	17	-1.50E-04
4	1.25E-05	18	-1.62E-04
5	0.0	19	-1.75E-04
6	-1.25E-05	20	-1.88E-04
7	-2.50E-05	21	2.00E-04
8	-3.75E-05	22	-2.12E-04
9	5.00E-05	23	-2.25E-04
10	6.25E-05	24	-2.38E-04
11	7.50E-05	25	-2.50E-04
12	8.75E-05	26	-2.62E-04
13	-1.00E-04	27	-2.75E-04
14	-1.12E-04		

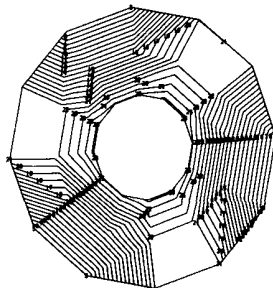
EACH CONTOUR REPRESENTS:  
12.5 micronsches (317 nanometers) change in figure,  
Half a wavelength in HeNe laser light, and  
The center of a bright band under a test plate  
illuminated with HeNe light

100% HE NE LASER ILLUMINATION  
STATIC DEFOR. SURFACE 1 LAMB 300

Figure 9. Surface figure loss caused by deformed flange (HeNe Illumination).

the boresite shift and figure changes are acceptable. Although this is a relatively coarse model to accurately resolve stresses, the order of magnitude of stresses in the structure and components can be determined. In this case, no permanent distortion of the structure will occur. Figure 10 shows the loss of surface figure in the primary mirror under 100 gs acceleration along the optical axis. Each dark contour line represents a dark band under a surface test plate as observed with HeNe illumination.

16 7/23/65 HRL-207 - 0.0000000



SYMBOL	VALUE (INCHES)	SYMBOL	VALUE (INCHES)
1	5.00E-05	15	-1.25E-04
2	3.75E-05	16	-1.38E-04
3	2.50E-05	17	-1.50E-04
4	1.25E-05	18	-1.62E-04
5	0.0	19	-1.75E-04
6	-1.25E-05	20	-1.88E-04
7	-2.50E-05	21	-2.00E-04
8	3.75E-05	22	-2.12E-04
9	-5.00E-05	23	-2.25E-04
10	-6.25E-05	24	-2.38E-04
11	7.50E-05	25	-2.50E-04
12	8.75E-05	26	-2.62E-04
13	1.00E-04	27	-2.75E-04
14	1.12E-04		

EACH CONTOUR REPRESENTS:  
12.5 micronsches (317 nanometers) change in figure,  
Half a wavelength in HeNe laser light, and  
The center of a bright band under a test plate  
illuminated with HeNe light

100% HE NE LASER ILLUMINATION  
STATIC DEFOR. SURFACE 3 LAMB 300

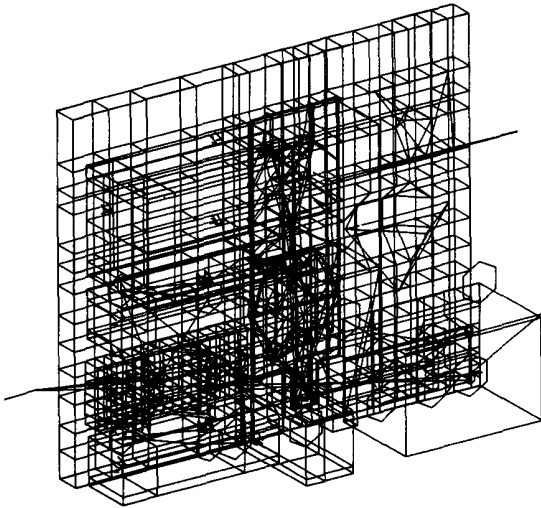
Figure 10. Surface figure loss caused by 100 g acceleration (HeNe Illumination).

### A large system optical bench

Another example is a model of a large optical system which is composed of three optical sub-systems mounted on an epoxy-graphite optical bench (Figure 11). In all, there are five optical paths sharing a common apperature. The boresite and alignment stability requirements make this a microradian class system. Boresite and alignment among the five optical paths had to be maintained in a variety of gravitational and transient thermal conditions. This analysis requires the solution of the system's steady state and transient heat transfer conditions in the finite element model. The temperature distributions are then used as static loads to solve for the thermal distortions of the structure. Chief rays for each of the optical paths are modeled by the procedure presented above. The angular deflection of the chief rays caused by structural distortion is used to indicate the boresite and alignment stability. Figure 12 is a MSC/NASTRAN plot of the five chief rays against an outline of the optical bench. Further reiterations of this model and use of features such as Design Sensitivity Analysis define a rational procedure for optimizing technical performance: in this case, the minimum weight system is desired which can maintain acceptable boresite and alignment stability.

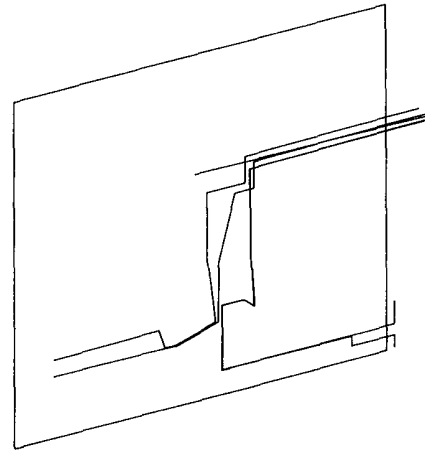
ALL SUBSYSTEMS ON THE OPTICAL BENCH

CHIEF RAY PATHS (5) - DEF - 0 07718230



VIEW OF THE OPTICAL BENCH  
STATIC DEFORM SUBCASE 7

Figure 11. Large optical system and optical bench.



VIEW OF THE OPTICAL BENCH  
STATIC DEFORM SUBCASE 7 LOAD 23

Figure 12. Deflected paths of chief rays in a large optical system.

### Conclusions

The finite element method is a very useful tool in evaluation optical and optomechanical system performance. A variety of optical phenomena can be included in finite element models and quantitatively evaluated in the solution process. Using sophisticated software, such as MSC/NASTRAN, the types of problems which may be analyzed is limited largely by the ingenuity of the analyst.

### References

1. Hatheway, A.E., Evaluating Optical System Performance with MSC/NASTRAN, Proceeding of the MSC/NASTRAN Users Conference, March 1984.